radiation

MDPI

Article

Minibeam Spatially-Fractionated Radiation Therapy Is Superior to Uniform Dose Radiation Therapy for Abscopal Effect When Combined with PD-L1 Checkpoint Inhibitor Immunotherapy in a Dual Tumor Murine Mammary Carcinoma Model

Judith N. Rivera [1], Keith Laemont [2], Artak Tovmasyan [3], Stefan Stryker [4], Kenneth Young [5], Theresa Charity [5], Gregory M. Palmer [4,5,*] and Sha Chang [6,7,*]

1 Department of Radiation Oncology, Indiana University School of Medicine, Indiana University, Indianapolis, IN 46202, USA; jrivera10@iuhealth.org
2 Clinical & Translational Science Institute, School of Medicine, Duke University, Durham, NC 27710, USA
3 Department of Translational Neuroscience, Ivy Brain Tumor Center, Barrow Neurological Institute, Phoenix, AZ 85013, USA; artak.tovmasyan@barrowneuro.org
4 Medical Physics Graduate Program, Duke University, Durham, NC 27705, USA
5 Department of Radiation Oncology, Duke Cancer Institute, Duke University, Durham, NC 27710, USA; kenneth.young@duke.edu (K.Y.); theresa.charity@duke.edu (T.C.)
6 Department of Biomedical Engineering, A Joint Program of the University of North Carolina-Chapel Hill and North Carolina State University, Chapel Hill, NC 27599, USA
7 Department of Radiation Oncology, Lineberger Comprehensive Cancer Center, School of Medicine, University of North Carolina-Chapel Hill, Chapel Hill, NC 27599, USA
* Correspondence: greg.palmer@duke.edu (G.M.P.); sha_chang@med.unc.edu (S.C.); Tel.: +1-(919)-613-5053 (G.M.P.); +1-(984)-974-8423 (S.C.)

Simple Summary: Minibeam radiation therapy is a novel approach to delivering radiation therapy in which a grid or other pattern is applied consisting of regions of high and low radiation dose. This is theorized to induce a strong immunogenic response by killing tumor cells receiving high dose, while sparing tumor infiltrating immune cells in the adjacent tissue. This has also been shown to have normal tissue sparing effects. This paper studies the combination of minibeam radiation therapy with immune checkpoint blockade to establish the therapeutic benefit of this approach.

Abstract: Spatially fractionated radiation therapy (SFRT) has a long history of treating bulky and hypoxic tumors. Recent evidence suggests that, compared to conventional uniform dose radiation therapy, SFRT may utilize different mechanisms of tumor cell killing, potentially including bystander and immune-activating effects. The abscopal effect in radiation therapy refers to the control or even elimination of distant untreated tumors following the treatment of a primary tumor with radiation, a process believed to be immune-mediated. Such effects have been shown to be enhanced by immunotherapy, particularly immune checkpoint inhibition. In this manuscript, we explore the potential synergy of spatially fractionated radiation therapy, in the form of kV x-ray minibeam, combined with PD-L1 checkpoint inhibition in a murine mammary carcinoma model at conventional dose-rate. We found that minibeam of peak/valley doses of 50 Gy/3.7 Gy performed statistically equivalent but trending better than that of 100 Gy/7.4 Gy in its abscopal effect and so 50 Gy/3.7 Gy was selected for further studies. Our findings indicate that the abscopal effect is significantly greater in the minibeam plus anti-PD-L1 treated animals compared to those receiving uniform dose radiation therapy plus anti-PD-L1 (p = 0.04948). Immune cell profiling in the minibeam plus anti-PD-L1 group compared to uniform dose reveals a consistent trend towards greater immune cell infiltration in the

check for updates

Academic Editor: Giusi Irma Forte

Received: 1 October 2024
Revised: 23 December 2024
Accepted: 28 December 2024
Published: 2 January 2025

Citation: Rivera, J.N.; Laemont, K.; Tovmasyan, A.; Stryker, S.; Young, K.; Charity, T.; Palmer, G.M.; Chang, S. Minibeam Spatially-Fractionated Radiation Therapy Is Superior to Uniform Dose Radiation Therapy for Abscopal Effect When Combined with PD-L1 Checkpoint Inhibitor Immunotherapy in a Dual Tumor Murine Mammary Carcinoma Model. *Radiation* **2025**, *5*, 3. https://doi.org/10.3390/radiation5010003

Copyright: © 2025 by the authors. Licensee MDPI, Basel, Switzerland. This article is an open access article distributed under the terms and conditions of the Creative Commons Attribution (CC BY) license (https://creativecommons.org/licenses/by/4.0/).

primary tumor, as well as a higher percentage of CD8+ T cells, both systemically and at the abscopal tumor site.

Keywords: radiation therapy; immune therapy; minibeam radiation therapy; spatially fractionated radiation therapy; immune checkpoint inhibitor

1. Introduction

Spatially fractionated radiation therapy (SFRT) is an unconventional radiotherapy approach to achieve high therapeutic index treatment, especially for hard-to-treat cases by conventional radiation therapy including tumors that are bulky and treatment resistant [1,2]. SFRT radiotherapy can be characterized by alternating high-dose (peaks) and low-dose (valleys) subregions within the tumor volume, in contrast to conventional radiotherapy which aims for tumor dose uniformity. Today SFRT encompasses various treatment approaches, including clinical SFRT using GRID and Lattice therapy (LRT) and preclinical SFRT using microbeam and minibeam using a variety of radiation sources including kV and MV x-rays, protons and particles [2–4].

Clinical SFRT using GRID and Lattice therapy have shown promising results in treating bulky and treatment-resistant tumors, effectively managing these challenging cases without increasing treatment toxicity [5–8]. These approaches provide significant benefits in terms of palliation and local control, particularly when combined with a conventional course of chemoradiation [7,9–12]. Preclinical SFRT research using microbeam and minibeam have also demonstrated promising outcomes, with much reduced radiation toxicity and effective tumor control [2,13–16].

Microbeam SFRT involves using extremely narrow, high-intensity beams of radiation, typically in the 10 s of micrometer range. Whereas minibeam utilizes larger beam typically 0.5–1 mm in size, usually spaced 1.5 to 4 mm apart [17]. Both techniques create a pattern of high-dose regions (beams) separated by low-dose regions (valleys) but the larger size minibeam is closer to the possibility of clinical application and thus draws increasingly more attention from researchers recently [18,19]. In minibeam SFRT, peak doses as high as 100 Gy were reported to be well tolerated [20,21]. It should be noted that toxicity is observed at 150 Gy or above peak dose depending on the beam width [21]. Preclinical studies to date have shown that minibeam offers remarkable normal tissue sparing [22–26] even at average doses of 20 Gy in a single fraction [18,27]. Both microbeam and minibeam expand the therapeutic window for aggressive tumor models in preclinical experiments. Minibeam has been shown to ablate radioresistant tumors with peak doses of 50–80 Gy, whereas microbeam requires hundreds of Gy to produce the same effect. [2]. The minibeam's potential as an effective and less damaging cancer treatment modality is supported by a recent initial report on a clinical study reporting successful treatments of bulky superficial tumors using kV x-ray minibeam [19].

Several studies on minibeam SFRT have reported equivalent or even superior tumor control compared to conventional uniform irradiation [16,28–31]. In a study by Bertho et al., up to 83% of tumor eradication in glioma bearing rats was observed despite using heterogeneous dose distributions contradicting the paradigm of conventional RT [31]. In general, SFRT challenges the conventional radiation therapy paradigm that lethal doses must be deposited in each tumor cell to eliminate the tumor, suggesting that other distinct biological mechanisms are activated [17]. However, the underlying biological mechanisms in SFRT, including minibeam, remain unclear.

Although SFRT research and clinical use have decades of history, it remains an unconventional treatment with limited although increasing clinical application. One key reason for this is the lack of understanding of SFRT's working mechanism. This not only impacts its wide acceptance in the field but also hinders the optimization of SFRT treatment techniques. In 2018, the National Cancer Institute partnered with the Radiosurgery Society to create a new international working group dedicated to investigating SFRT and the related Flash radiotherapy [1]. The working group was tasked to develop strategies to guide the field to advance our understanding of SFRT in biology, physics, and clinical translation of this promising radiation therapy approach. One area of special interest deserving more research is the SFRT-induced abscopal effect. Emerging evidence suggests that SFRT, including microbeam and minibeam, can stimulate an immune response against tumors. The localized high-dose regions can induce immunogenic cell death, potentially enhancing the systemic anti-tumor immune response [32].

SFRT may offer advantages in enhancing anti-cancer immunotherapy compared to the uniform dose radiation therapy currently in routine use. SFRT can result in unique effects on the tumor microenvironment, potentially leading to different mechanisms of cell killing, such as bystander effects [33,34] and effects on stromal cells, including the tumor vasculature [35–39]. Notably, radiation-induced immunological effects can lead to abscopal or distant tumor responses, which have been reported in various contexts involving SFRT with and without immune therapies [40–44]. For instance, Kanagavelu et al. reported significant growth inhibition in distant unirradiated Lewis lung carcinoma mouse tumors following partial volume radiation of a primary tumor, correlated with a T-cell mediated immune response [44]. Clinical data also supports the efficacy of partial volume irradiation targeting hypoxic tumor regions, a unique form of SFRT, to elicit an immune-mediated abscopal response [45].

The combination of SFRT with immunotherapies has also shown potential for better synergy relative to the conventional uniform dose radiation therapy [40–44]. The coexistence of both high dose and low dose subregions in the tumor may induce unique effects by sparing a fraction of the resident immune population while in the high dose subregions releasing tumor-specific antigens and attracting chemokines to activated T-cells, thus engaging the patient's innate immune response against the tumor [43], which could elicit the in-situ vaccination effect reported for uniform radiotherapy [46]. Several clinical studies have indicated that "the tumor can serve as an autologous vaccine through RT-induced immunogenic cancer cell death" [47]. This suggests that the radiation itself may activate or enhance the host immune response against future metastatic tumor cells, potentially leading to significantly better long-term prognoses for patients [47–53]. A study by Bertho et al. [17] was the first to demonstrate long-term anti-tumor immunity activation following minibeam in an orthotopic glioma model. The research revealed an average increase in T-cell density by 11-fold in the conventional treatment group and 13-fold in the minibeam group. These results indicate the development of an adaptive immune response within the tumor tissue. We hypothesize that, compared to conventional uniform dose radiation therapy, SFRT, specifically minibeam, is superior in inducing a systemic immune response that can target distant (unirradiated) tumor sites.

Despite the tremendous promise of this SFRT and immunotherapy combination, the specific immune responses that SFRT elicits are not well understood. The goal of this study is to characterize and compare the efficacy of combining radiation (either minibeam or uniform radiation) with anti-PD-L1 immunotherapy. Additionally, the study uses flow cytometry to analyze the immune cells present in the primary irradiated tumor, distant unirradiated tumor, and systemically throughout the body.

2. Methods

2.1. Study Design

This study was designed to investigate the synergistic impact of immune checkpoint inhibitor therapy when combined with x-ray minibeam SFRT at two dose levels and conventional uniform dose radiation therapy. There are two segments in the study. The first is Minibeam Dose Determination Study to determine the proper dose level to use to best induce an abscopal effect when combined with immune checkpoint inhibitor therapy. The second segment is Comparative Treatment Study with the aim to compare the abscopal effect of minibeam versus uniform radiation when combined with immune checkpoint inhibitor therapy.

A research irradiator is used to generate all radiation beams in this study. An in-house fabricated minibeam collimator is used on the irradiator to convert the uniform radiation to minibeam radiation, the details of which have been described in our previous publication [54]. All radiation treatments are delivered in a single fraction, followed by either an immune checkpoint inhibitor therapy drug or an isotype antibody control.

2.2. Minibeam Dose Determination Study

We hypothesize that the modulation of host's anti-tumor immune response is minibeam dose dependent. To test this hypothesis, we compared 50 Gy/3.7 Gy and 100 Gy/7.4 Gy (peak/valley doses) minibeams in terms of local control of the treated tumor and the abscopal effect on the untreated tumor in a dual tumor mouse model of adenocarcinoma. A single fraction minibeam was delivered to one of the two tumors. For each of the minibeam dose groups, two groups of animals were used: one with the immunomodulator, anti-PD-L1 antibody, and one without. An isotype control was given to the no immunomodulator groups. Additionally, a control group receiving no radiation treatment and an isotype control was used. The primary endpoint for this study was tumor growth inhibition at both the irradiated and unirradiated tumor sites.

2.3. Comparative Treatment Study

Following the minibeam dose determination study, we conducted a comparative treatment study between minibeam radiation and the conventional uniform dose radiation. We hypothesize that, minibeam radiation spatial fractionation in tumor plays an important role in potentiating the immunotherapeutic abscopal effect. To test this hypothesis, we compared 50 Gy/3.7 Gy (peak/valley dose) MinibeamRT and 10 Gy UniformRT treatments in terms of local control of the treated tumor and the abscopal effect on the untreated tumor. The calculated volume-averaged tumor dose for the MinibeamRT group is 11.1 Gy, which is 17% higher than that of the UniformRT group (9.2 Gy). For each radiation treatment type, two groups of animals were used: one group received the immune checkpoint inhibitor, anti-PD-L1 antibody, and the other group received an isotype control. Additionally, a control group received no radiation treatment and an isotype control. The primary endpoint for this study was tumor growth inhibition at both the irradiated and unirradiated tumor sites.

In Table 1, the 5 treatment groups designed for this study are summarized along with pre-treatment tumor volumes in both flanks.

Initial tumor size at the time of treatment has shown a strong correlation with treatment outcome in preclinical studies. To mitigate any potential influence of initial tumor size differences among treatment groups, particular attention was given to ensuring uniformity in pre-treatment tumor volumes, especially in the right flank tumors used for treatment allocation. To achieve this, animals were grouped based on similarly sized right flank tumor volumes, and then randomly assigned to each treatment arm within these size-matched categories. This approach resulted in comparable average pre-treatment tumor volumes and

size ranges among different treatment groups on the right flank. However, since there is no control over the volumes in the left flank untreated tumors per group, steps were taken to minimize variance among pre-treatment tumor volumes in the left flank. This included setting minimum and maximum acceptable pre-treatment volume limits and excluding any tumor volumes outside of this range from consideration in the study. As a result of this randomized, matched study design technique, the average pre-treatment tumor volume for all right flank tumors was approximately 124 mm^3 (±7% standard error), while the average pre-treatment tumor volume for all left flank tumors was 132 mm^3 (±8% standard error).

Table 1. Experimental design of seamless (UniformRT) vs. spatially fractionated (MinibeamRT) radiation therapy study of the systemic immune response of mice.

Treatment Groups	Animal Numbers (n = 59)	Dose [a] (Gy)	Pre-Treatment Tumor Volumes [d]	
			Right (Irradiated)	Left (Unirradiated)
Controls + isotype [c]	15	0	140.7 (±25%)	146.8 (±19%)
UniformRT + isotype	11	10	124.3 (±12%)	141.0 (±13%)
UniformRT + α-PD-L1	12	10	118.3 (±14%)	115.9 (±17%)
MinibeamRT + isotype	11	50 [b]	121.2 (±13%)	122.0 (±15%)
MinibeamRT + α-PD-L1	10	50 [b]	117.0 (±13%)	133.0 (±23%)

[a]: Dose is measured using EBT-3 film at the phantom surface. For MinibeamRT treatments the dose in the peak regions is used. For more dosimetry information, see Table 2. [b]: Approximately n = 5 animals for each treatment group were harvested for flow cytometry immune profiling. [c]: Controls + isotype treatment arm animals received no radiation to either tumor. [d]: Average tumor volume (±%standard-error) reported for each treatment group.

Table 2. Key dosimetry parameters used in the study. Dosimetry is measured on mouse-sized phantom.

Treatment Arm	Vol-Avg Dose [a] (Gy)	Peak Surface Dose [b] (Gy)	Valley Surface Dose [c] (Gy)	PVDR at Surface	Valley Width (mm)	Peak Width (mm)
Controls	0	0	0	N/A	N/A	N/A
10 Gy UniformRT	9.2	10	10	1	20	20
50 Gy MinibeamRT	11.1	50	3.8	13.3	0.9	0.31
100 Gy MinibeamRT	22.2	100	7.5	13.3	0.9	0.31

[a] Volume-averaged dose is calculated through a 10 mm depth (approx. maximum tumor depth). [b,c] Peak and valley dose are calculated at 0 mm depth (to the skin surface).

2.4. Animal Model Description and Cell Culture

This study adhered strictly to the recommendations outlined in the Guide for the Care and Use of Laboratory Animals of the National Institutes of Health (NIH). The University of North Carolina-Chapel Hill Institutional Animal Care and Use Committee (IACUC) reviewed and approved the animal protocol (IACUC ID: 19–041.0) in accordance with NIH standards. All animal radiation procedures were conducted under general anesthesia, and all efforts were made to minimize any potential suffering.

For the experiments, a dual-tumor model was utilized involving 6-week-old female C57BL/6 mice with murine mammary adenocarcinoma (EO771). These cells were derived from a metastatic mammary gland adenocarcinoma in a C57BL/6 mouse [55–57], chosen for its immune competence and relevance to clinical studies, particularly in studying radiotherapy-induced tumor microenvironment modulation effects [58]. This mammary gland adenocarcinoma model is characterized as a poorly metastatic, triple-negative model of breast cancer.

Tumor cells were cultured in DMEM supplemented with 10% FBS (Gibco 16140071) and 1% antibiotic-antimycotic (Gibco 15240062). Subsequently, cells were injected into the subcutaneous space of both flanks of the mice: the right flank received 250,000 cells, and the left flank received 100,000 cells.

Figure 1 provides a graphical timeline of the experiment. Tumors on both flanks were allowed to grow naturally for approximately 2 weeks until the primary tumor reached

the target radiotherapy treatment size of approximately 120 mm^3. The right flank tumors served as the "primary" tumor for targeted radiation therapy, while the left flank tumors served as the "secondary" tumors outside the radiation field to evaluate the abscopal (unirradiated tumor growth control) response. Following the radiotherapy treatments, animals received injections of anti-PD-L1 monoclonal antibody (BioXCell clone 10F) or an isotype control antibody (IgG2a) immediately. The dose of antibody (250 µg) was based on previous mouse studies, administered via intraperitoneal injection every 3 days starting on the day of radiation treatment for a total of 4 injections. At 14 days post-radiotherapy, approximately n = 5 animals from each treatment group were humanely euthanized for immunophenotyping of spleen and both irradiated and unirradiated tumors, in accordance with the IACUC-approved animal protocol.

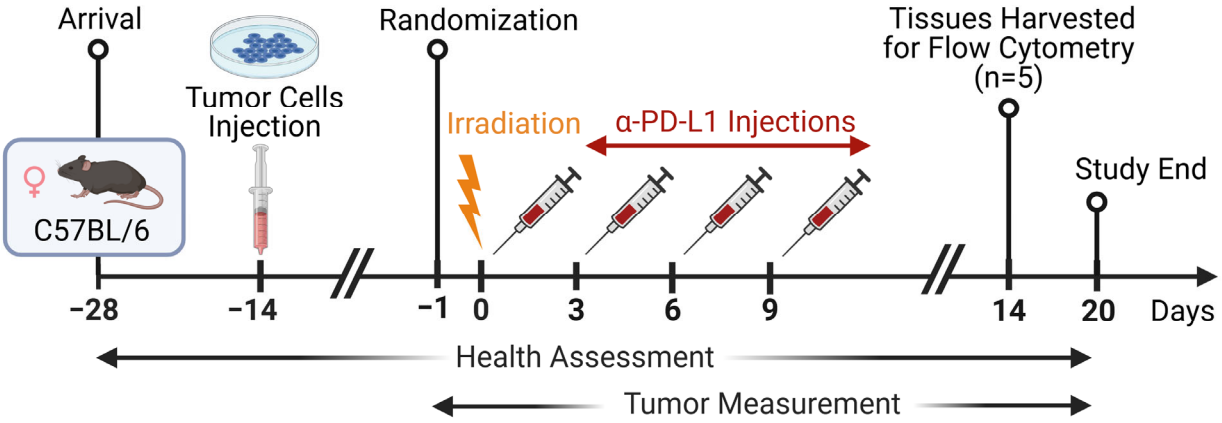

Figure 1. The timeline of the study is shown. A single fraction radiation is given two weeks after tumor cell implantation. Anti-PD-L1 immune drug was given in 4 fractions starting on day 0. On day 14 tissues are harvested from n = 5 animals per treatment group for flow cytometry immunophenotypic analysis. The remaining animals are monitored for tumor growth and the study ends on day 20.

Spleens were processed by homogenization using a syringe plunger and filtered through a 40 mm cell strainer (Corning, Corning, NY, USA, cat#431750). Red blood cells were lysed using lysis buffer (15.5 mM NH4Cl, 1.2 mM NaHCO3, 0.01 M EDTA). Tumor lymphocytes were isolated using a GentleMACS dissociator (Miltenyi Biotec, Bergisch Gladbach, Germany) in a solution of 0.2 mg/mL DNase I, 1 mg/mL collagenase IV, and 0.1 mg/mL hyaluronidase (Sigma, Burlington, MA, USA), incubated at 37 °C for 1 h, and then passed through a 40 µM strainer (Falcon, Wixom, MI, USA) to obtain single-cell suspensions. The cells were then stained with anti-CD16/32 Ab (BioLegend, San Diego, CA, USA) to block nonspecific binding and LIVE/DEAD Fixable Violet Dead Cell Stain Kit (Thermo Fisher, Waltham, MA, USA) to exclude dead cells. Subsequently, the cells were stained with antibodies against CD45, CD3, CD4, CD8, CD25, CD19, CD335, CD11b, F4/80, Gr1, and PD-1 (BioLegend, San Diego, CA, USA), and analyzed by multiparameter flow cytometry (FACSCanto, BD Bioscience, Franklin Lakes, NJ, USA). Data analysis was conducted using FlowJo software (Version 10, Tree Star, Ashland, OR, USA).

2.5. Animal Monitoring and Husbandry

Animals were monitored both prior to irradiation and every third day thereafter until they met study endpoint criteria. These criteria included a maximum combined tumor burden of 3000 mm^3 (or a single tumor exceeding 2 cm in any dimension), weight loss exceeding 15%, body condition scores of $\leq$2, and any signs of pain, discomfort, or moribundity as advised by DCM veterinary staff. Animals meeting these criteria were

humanely euthanized using compressed carbon dioxide gas followed by thoracotomy, in accordance with the approved animal study protocol.

Body weights and tumor volumes were documented before radiotherapy treatments and subsequently every third day for up to 30 days. Tumor dimensions were measured using a digital caliper, and tumor volumes were calculated using the formula for an oblate spheroid: V = (1/2) L × W × W, as recommended by Faustino-Rocha et al. [59].

To minimize biological variability across animals and experimental runs, all animals were of similar age and were sourced from the same vendor (Charles River Laboratories, Inc., Wilmington, MA, USA). They underwent a full 2-week acclimation period before the commencement of any treatments, received cell injections on the same day, and were housed under identical conditions in mixed cages at a UNC Division of Comparative Medicine (DCM) operated vivarium facility. Throughout the study, all animals were provided with standard laboratory rodent diets consisting of at least 23% crude protein and had access to water ad libitum. Additionally, to mitigate potential significant weight loss or dehydration following radiation exposure, all animal diets were supplemented with high-calorie, nutritionally fortified water-based gel and hydration cups.

2.6. Radiotherapy Dosimetry and Treatments

Radiotherapy treatments were administered using the XRad-320, a commercially available small animal research irradiator from Precision XRay, Inc. (North Branford, CT, USA), operating at 320 kVp and 12.5 mA. In-house-made collimators were employed to deliver both collimated MinibeamRT and UniformRT radiation patterns to solid tumors. Figure 2 illustrates (Figure 2A) beam profile and percentage depth dosimetry measurements for MinibeamRT and UniformRT treatments, (Figure 2B) the setup of the small animal radiotherapy treatment system, and (Figure 2C) an example image of a mouse treated with 10 Gy UniformRT.

Dosimetry for radiotherapy was assessed using EBT-3 Gafchromic film from Ashland Inc. (Covington, KY, USA), calibrated against an ADCL-certified ion chamber in large-field geometry. Table 2 details dosimetric parameters for both UniformRT and MinibeamRT treatment arms, derived from dosimetry film (Figure 2A). Surface peak and valley doses for MinibeamRT were calculated by averaging individual peak and valley doses within a 10 mm span around the center of the MinibeamRT field. The surface dose rates were determined to be 4.27 Gy/min for MinibeamRT and 5.25 Gy/min for UniformRT treatments, falling within the range typical of clinical conventional dose rate radiation therapy. Volume-averaged doses for both treatment types were approximated by averaging doses over a 10 mm (width) × 10 mm (depth) area on the percentage depth dose (PDD) dosimetry film. Table 2 shows the key dosimetric information (profiles and parameters) for the four radiation groups in this study.

Both the UniformRT and the MinibeamRT radiation fields were shaped using our in-house developed collimators described previously [54]. Treatment targeting involved (a) depilating animal flanks for tumor localization and marking tumor boundaries on the skin, (b) transferring these markings onto a 3 cm × 3 cm square of Gafchromic film for treatment verification, (c) cutting out the film section corresponding to the tumor and securing it over the tumor site, (d) fixing the film with tape and positioning the animal in the irradiator, (e) aligning the tumor within the radiation field using built-in light field and a PC-linked endoscopic camera for live video feed, (f) adjusting tumor position vertically via manual Z-stage and angular adjustments via a rotatable heated animal platform, and (g) monitoring the animal throughout irradiation using a second PC-linked endoscopic camera. In this study that focused on tumor response to radiation and its modulation to the tumor immune environment, the radiation fields used were not conformal. This is to

ensure the tumor radiation coverage is adequate in the research irradiator, which does not have the ability of clinical treatment machines for precise radiation targeting. Isoflurane (2%) mixed with oxygen carrier gas was used to maintain anesthesia during tumor-to-beam alignment and irradiation, ensuring minimal stress to the animals and reducing off-target errors due to tumor motion. Treatment verification films were used to confirm targeting accuracy post-radiation and for documentation purposes.

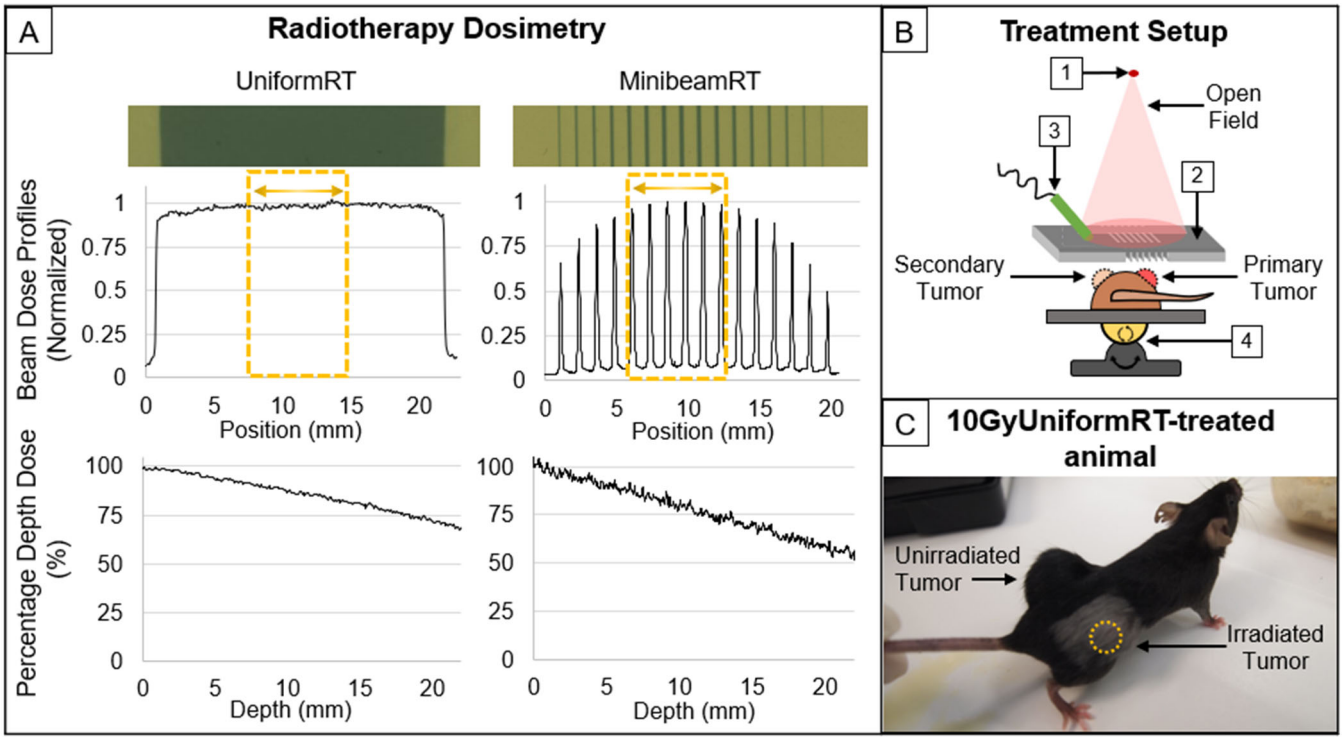

Figure 2. (**A**) Dosimetry beam profiles and percentage depth dose (PDD) for the UniformRT and MinibeamRT treatments by EBT-3 film. The yellow dotted rectangle represents the approximate size of a typical tumor at the time of irradiation and the position in the treatment field. (**B**) The radiation treatment setup includes (1) an external beam x-ray source, (2) an in-house Cerrobend MinibeamRT or UniformRT collimator, (3) a PC-linked camera provides beam's-eye-view of the light field on animal skin, and (4) a 6-degree freedom platform for angle and height adjustment. (**C**) image of an animal treated by 10 Gy UniformRT, photographed approximately 3 weeks post-radiation. A demarcated square patch of white fur is visible, corresponding to the radiation field, indicating a localized radiation-induced epidermal and fur depigmentation disorder (vitiligo). No abscopal effect is observed in this animal.

2.7. Flow Cytometry Studies Description and Analysis Methods

At 14 days post-radiation, approximately n = 5 animals from each treatment group were ethically euthanized, and spleens as well as both irradiated and unirradiated tumors were harvested for immune profile analysis according to the IACUC-approved protocol. Flow cytometry was utilized to assess the prevalence of different immune cell subtypes within these tissues. Fluorescent-labeled antibodies targeting specific cell surface markers were employed to identify distinct immune cell populations.

CD45, known for its role in regulating T-cell and B-cell antigen receptor signaling, was used as a key marker for leukocytes. Cells expressing high levels of CD45 were quantified through thresholding. To further classify the leukocyte population into primary subtypes, three additional markers were utilized. CD3, expressed by a significant proportion of circulating peripheral T cells, served as a marker for T cells and aided in further subtyping of CD45+ leukocytes. CD4, a glycoprotein found on immune cells like T helper cells (Th

cells), was used to identify T-helper cell populations in our study. Additionally, CD8, predominantly expressed on cytotoxic T cells (Tc cells) and natural killer (NK) cells, was employed as a marker for cytotoxic T cells. Thus, cells expressing both CD3 and CD4 were categorized as helper T cells, while those expressing CD3 and CD8 were classified as cytotoxic T cells.

3. Results

3.1. Minibeam Dose Determination Study: 50 Gy Peak Dose Minibeam Is More Effective than 100 Gy Peak Dose Minibeam for Abscopal Effect

In a pilot experiment for minibeam dose determination we compared the local and abscopal tumor control post radiation for 7 treatment groups including the 50 Gy and 100 Gy peak dose MinibeamRT groups as well as the 10 Gy uniform radiation and no radiation control group with and without anti-PD-L1 drug. Figure 3 shows the treatment response for both the treated and untreated tumor with and without the immune checkpoint inhibitor drug anti-PD-L1 for the 7 treatment groups. The pilot data indicated that the anti-PD-L1 enhanced tumor control for both the treated and untreated tumor in practically all groups studied, especially for the 50 Gy peak dose minibeam group. For the minibeam groups, the 50 Gy peak dose may initiate stronger abscopal effect than the 100 Gy peak dose, while latter may be superior that the former in treated tumor control. Compared to both the minibeam groups, the 10 Gy uniform dose group had the best treated tumor local control, and this finding is consistent with our experience in previous minibeam preclinical studies [54]. Based on this result, we decided to use the 50 Gy peak dose minibeam and uniform radiation of similar average dose to study the impact of radiation spatial fractionation on radiation immune modulation.

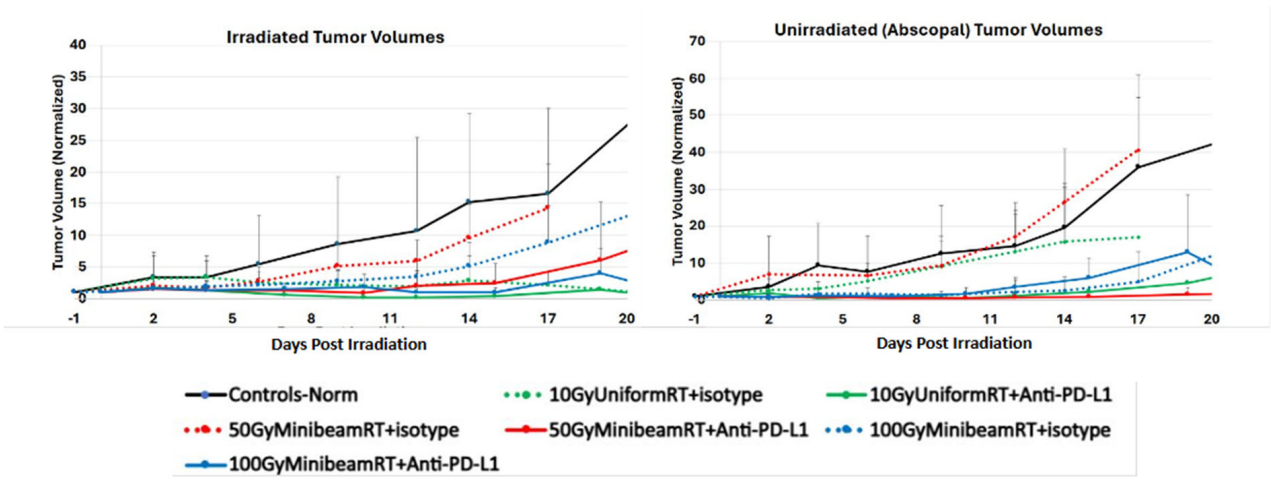

Figure 3. Normalized tumor volume change post radiation is shown for both the irradiated tumor (**left**) and the unirradiated tumor (**right**) in the dual tumor animal model study.

3.2. Comparative Treatment Study: 50 Gy Peak Dose MinibeamRT Is More Effective than 10 Gy UniformRT of Similar Average Dose for Abscopal Effect When Paired with Anti-PD-L1

(A.) Irradiated Tumor Response: Figure 4A shows results for normalized tumor volume growth curves for the irradiated "primary" tumors. Ethical euthanasia was largely triggered by tumors exceeding the maximum combined tumor burden for both tumors per IACUC-approved protocol limitations. Skin ulceration occurred in some animals due to tumor growth, but did not appear to be treatment related. Some whitening of the fur at the site of irradiation was observed in all irradiated groups. Our data shows that conventional UniformRT groups (10 Gy surface dose and 9.2 Gy average dose to tumor), with or without anti-PD-L1 drug, have better tumor growth control than the corresponding

50 Gy MinibeamRT arms (50 Gy surface peak dose and 11.1 Gy average dose to tumor.) The observed impact of anti-PD-L1 on the treated tumor control is statistically insignificant for both the minibeam and uniform RT treatments.

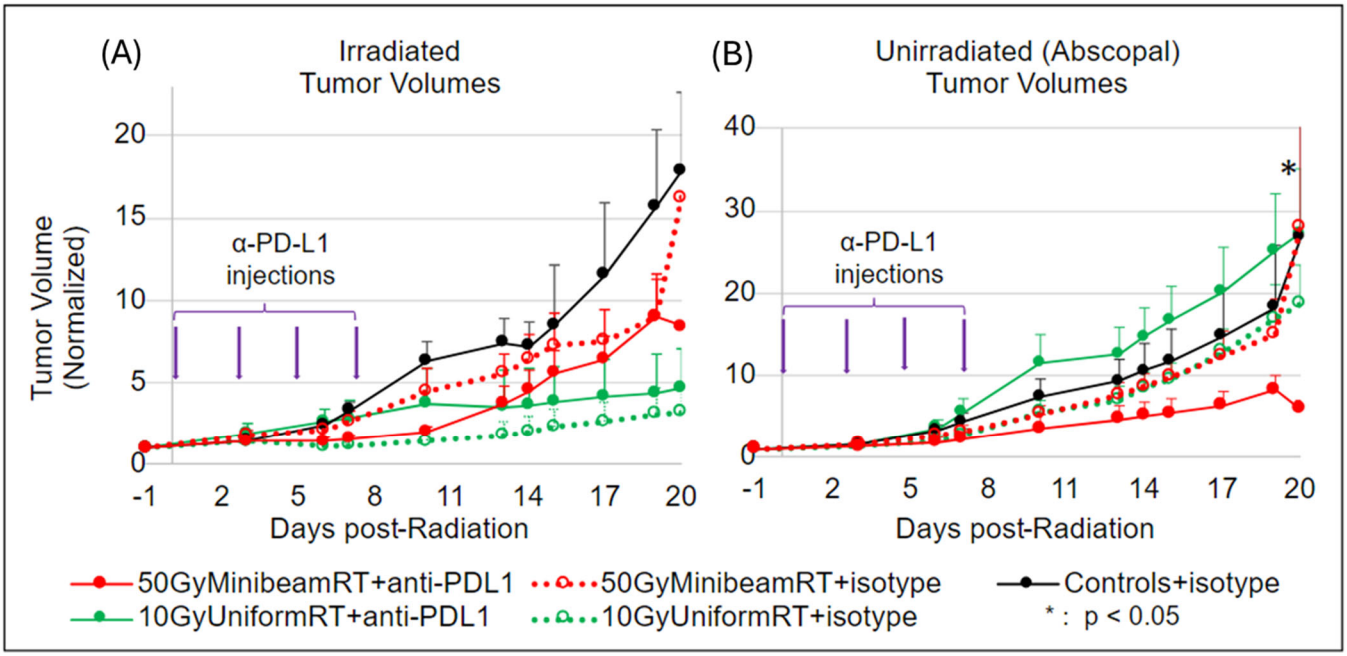

Figure 4. Normalized tumor volume change post radiation is shown for both the irradiated tumor (**A**) and the unirradiated tumor (**B**) in the dual tumor animal model study. For the unirradiated abscopal tumor, the difference between the 10 Gy UniformRT + anti-PDL1 and the 50 Gy MinibeamRT + anti-PDL1 treatment groups at the end of study is statistically significant ($p = 0.04948$). Differences between any other two groups are not statistically significant in this study.

(B.) Unirradiated Tumor Response (Abscopal Effect): Figure 4B shows results for normalized tumor volume growth curves for the unirradiated tumor. In the absence of anti-PD-L1 drug the UniformRT and the 50 Gy MinibeamRT radiation treatment to the primary tumor have practically no impact on the secondary, unirradiated tumor, whose growth curves are similar to those of the control arm animals. When anti-PD-L1 is combined with the radiation, the MinibeamRT radiation exhibits the strongest abscopal effect, where the growth of the unirradiated tumor is significantly reduced, especially when compared to the UniformRT + anti-PD-L1 arm ($p = 0.04948$). Further, the combination of anti-PD-L1 with UniformRT radiation appears to generate a negative abscopal effect, where the tumor growth is enhanced compared to uniform radiation alone. The difference between the 10 Gy UniformRT + anti-PDL1 and the 50 Gy MinibeamRT + anti-PDL1 treatment groups at the end of study is statistically significant ($p = 0.04948$).

3.3. Spleen Lymphocyte Profile

In the 50 Gy MinibeamRT and 10 Gy UniformRT groups, some of the animals were sacrificed on day 14 and tumors and spleens were harvested for flow cytometry analysis. Figure 5 shows the T cell flow cytometry immune profiling data from the spleen. We analyzed CD45+, CD3+, CD4+, and CD8+ cells. A few clear differences are seen. Firstly, the CD4+ cell population is similarly elevated for both the MinibeamRT + isotype and UniformRT + isotype arms ($p = 0.01322$) compared to controls. The CD4+ populations are similar for the anti-PD-L1 with RT-treated animals, which are very similar and not statistically significantly different from the control arm. Secondly, a similar but inverse trend is seen for the CD8+ cells. The RT + anti-PD-L1 drug combination treated animals

retained their CD8+ cell population percentages compared to controls. However, the RT-alone (without anti-PD-L1 drug) treated animals showed significantly lowered levels compared to controls (p = 0.02685 for UniformRT + isotype arm; p = 0.0256 for the MinibeamRT + isotype arm).

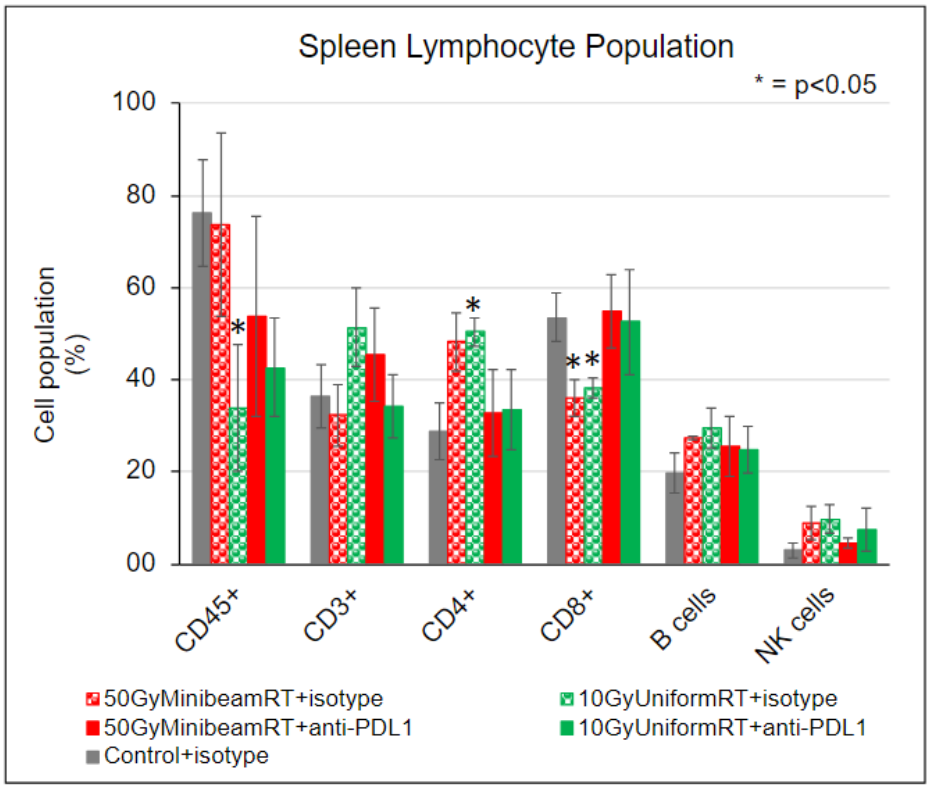

Figure 5. Flow cytometry immunophenotypic analysis of spleen cells that are harvested at 14 days post-radiotherapy. Approximately five animals per study group are harvested and thresholding was applied to categorize cells based on immunofluorescence signal levels. When statistically compared against the Control + isotype arm, the 10 Gy UniformRT + isotope arm is significantly different for CD45+ (p = 0.04378), CD4+ (p = 0.01322), and CD8 (p = 0.02685). In addition, for CD8 cells the 50 Gy MinibeamRT + isotope arm is significantly different from Control + isotype (p = 0.0256).

3.4. Tumor Lymphocyte Profiles

Figure 6 shows the flow cytometry immune profiling data from both the irradiated and unirradiated tumors, where CD3+, CD8+, and CD4+ cell population percentages are analyzed. For the irradiated tumor, UniformRT alone (without anti-PD-L1) appears to cause the greatest depletion of the overall T-cell population (CD3+), while the MinibeamRT alone arm maintains a CD3+ population nearly the same as the control arm. This suggests that MinibeamRT might spare some fraction of the resident lymphocyte population. The anti-PD-L1 drug enhanced the resident T-cell population in both radiation groups, especially for the UniformRT group.

For the distant unirradiated tumor, there is no clear difference among the immune cell populations. However, there appears to be a trend towards higher CD8+ cytotoxic T cells in the 50 Gy MinibeamRT + anti-PD-L1 group, indicating greater anti-tumor immune activity. This trend is consistent with the spleen data, where the 50 Gy MinibeamRT + anti-PD-L1 group had the highest CD8+ T cell population among the irradiated animals, suggesting a greater systemic CD8+ T cell response. This systemic response is a critical determinant of the anti-tumor effect in several models. These observed trends support our hypothesis that MinibeamRT induces and enhances a systemic immune response. However, the relatively

large within-group variance and the exploratory nature of this study do not allow us to establish statistical significance between the groups.

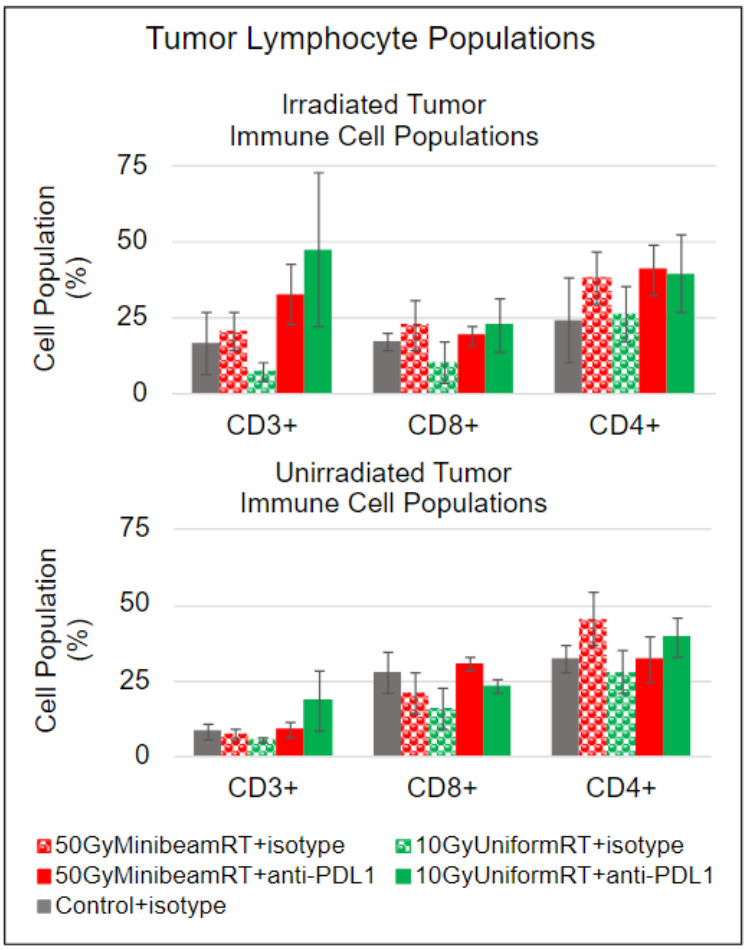

Figure 6. Flow cytometry immunophenotypic analysis of cells harvested from the irradiated tumor (**top**) and unirradiated tumors (**bottom**) of a dual tumor mouse model of adenocarcinoma. Tumors were harvested from approximately n = 5 animals per treatment group at 14 days and thresholding was applied to categorize cells based on immunofluorescence signal levels.

4. Discussion

In this study we aim to investigate the impact of radiation spatial fractionation in the form of minibeam on host tumor radiation-induced immune modulation with and without immune checkpoint inhibitor drug anti-PD-L1 in a dual tumor murine model. We observed the treatment responses in both the treated and the untreated abscopal tumors and performed immune profile analysis for some animals from each of the study groups. Our study suggests that lower, not higher, dose may be preferred in minibeam treatment to elicit abscopal effect when combined with anti-PD-L1 therapy. We have shown that the 50 Gy/3.7 Gy peak/valley dose MinibeamRT trended better than 100 Gy/7.4 Gy MinibeamRT in eliciting an abscopal effect on the untreated tumor. This finding is consistent with the idea that the valley dose should be below 5 Gy to preserve tumor-infiltrating immune cells, including antigen-presenting cells, which are essential for the radiation-vaccination in situ effect [60–62]. The 50 Gy MinibeamRT treatment has a volume-averaged dose of 11.1 Gy, which is only 17% higher than that of the 10 Gy UniformRT treatment. Thus our study suggests that radiation spatial fractionation enhances checkpoint inhibitor immunotherapy and abscopal effect. Our tumor growth data shows that comparing to the 10 Gy UniformRT dose group of similar average dose plus anti-PD-L1 therapy, the

50 Gy MinibeamRT is more effective in abscopal tumor control. Although the 10 Gy uniform radiation showed the best treated tumor control among the 7 study groups it presented the least tumor control at the untreated abscopal tumor site, consistent with other studies indicating that single-dose uniform radiotherapy does not induce an abscopal tumor response [61,63]. However, the uniform radiation showed better control of the treated tumor, consistent with our previous observation in an animal study where uniform radiation is superior to minibeam radiation for similar average doses [54].

Our study indicates the potentially advantageous role of SFRT in the form of minibeam in eliciting a systemic anti-tumor immune response. This is supported by trends seen in the flow cytometry characterization of immune cell infiltrates. Notably, elevated CD8+ T cells were observed in the distant (unirradiated) tumor site and the spleen, indicating a greater systemic cytotoxic immune response. Additionally, overall T cell populations were elevated in MinibeamRT + anti-PD-L1 treated groups, suggesting greater retention of resident T cell populations, in line with our hypothesis. This is consistent with previous reports on the immune response following conventional radiation, where CD8+ T cell response is elevated following combined radiation and PD-1/PD-L1 blockade in mouse models of glioblastoma multiforme [64]. Deng et al. also showed that CD8+ T cells play a critical role in the response to UniformRT combined with immune checkpoint inhibition in a breast cancer mouse model [65]. Elevated CD8+ T cells are also a positive prognostic factor clinically, and immune checkpoint inhibition combined with radiation has been shown to increase the prevalence and activation of CD8+ T cell populations as an important mechanism of response [66,67]. Therefore, minibeam SFRT has a potential role in enhancing the immune response following combination therapy as discussed previously [40–44]. In this work, we chose to use anti-PD-L1 as an immune therapy because it has been shown to synergize with radiation therapy in various tumor models and is also being studied clinically. However, many other potential immune therapies have also been shown to be synergistic in combination with radiation therapy [68,69].

One significant challenge in all SFRT studies is the lack of understanding in the correlation between SFRT dosimetric parameters and a given treatment response [2,54,70]. Without the essential understanding we have little basis to optimize the large dosimetric parameter space of a SFRT treatment based on treatment response, which in this case is immune modulation. Our data indicates that a lower not higher minibeam dose is preferred in enhancing anti-PD-L1 drug and eliciting abscopal effect. Our study confirmed our previous finding [54] and clearly showed that tumor average dose has no correlation with treatment response. In the treated tumor, the 10 Gy uniform dose group with 9.2 Gy average dose is superior in tumor control than the 50 Gy MinibeamRT group with 11.1 Gy tumor average dose. In the untreated abscopal tumor, the 50 Gy MinibeamRT group is superior to the 10 Gy UniformRT group. We hypothesize that the spatial dose distribution in tumor may significantly affect the immune response, which is likely dependent on the tumor's specific microenvironmental properties. Clinical implication of our work is unclear as more studies are needed to understand how the spatial dose distribution affects the immune response in manners that are relevant to SFRT clinical application, which is very different than most SFRT used in preclinical studies in terms of spatial fractionation scale, pattern, dose, and temporal fractionation [2,71,72]. Some limitations of this study include the small sample sizes and heterogeneity of response, as reflective of the preliminary nature of these findings. This heterogeneity may be driven by a wide range of experimental conditions and individual tumor characteristics, including tumor size, perfusion, hypoxia, vascular permeability, and PD-L1/PD-1 expression. Additional studies are needed to confirm these findings and to better understand the mechanistic basis for the radiation and immune system responses.

5. Conclusions

Our study shows that while minibeam SFRT radiation is superior at initiating an abscopal effect, conventional uniform radiation at 17% lower average dose is better at treated tumor control. This is likely due to the much lower minimum tumor dose from the minibeam treatment compared to the uniform dose treatment. If validated, a strategy of minibeam SFRT plus conventional RT treatment, could be ideal to harness both the benefits of both the SFRT and uniform radiation therapy. The strategy would involve first using minibeam + anti-PD-L1 on a localized tumor to enhance systemic anti-cancer immunotherapy effect, and then 1–2 week later followed by conformal conventional radiation therapy for effective local tumor control. Minibeam with high PVDR is likely more effective in enhancing anti-cancer immunotherapy than GRID and Lattice SFRT with low PVDR. More studies are needed to confirm the finding of this work using different tumor models and explore the best timing for the combined minibeam and conventional radiation treatment approach.

Author Contributions: Conceptualization, S.C. and G.M.P.; methodology, J.N.R., K.L., A.T., S.S., K.Y., G.M.P. and S.C.; formal analysis, J.N.R., K.Y., G.M.P. and S.C.; investigation, J.N.R., K.L., A.T., S.S. and K.Y.; resources, S.C. and G.M.P.; writing—original draft preparation, J.N.R., G.M.P. and S.C.; writing—review and editing, J.N.R., T.C., G.M.P. and S.C.; visualization, J.N.R., K.Y., A.T. and T.C.; supervision, G.M.P. and S.C.; project administration, S.C.; funding acquisition, S.C. All authors have read and agreed to the published version of the manuscript.

Funding: This research received no external funding.

Institutional Review Board Statement: The study was conducted in accordance with the Declaration of Helsinki, and approved by the Institutional Review Board (or Ethics Committee) of The University of North Carolina-Chapel Hill Institutional Animal Care and Use Committee (IACUC) (protocol code IACUC ID: 19-041.0 (approved December 2017).

Informed Consent Statement: Not applicable.

Data Availability Statement: The raw data supporting the conclusions of this article will be made available by the authors on request.

Conflicts of Interest: The authors declare no conflicts of interest.

References

1. Griffin, R.J.; Ahmed, M.M.; Amendola, B.; Belyakov, O.; Bentzen, S.M.; Butterworth, K.T.; Chang, S.; Coleman, C.N.; Djonov, V.; Formenti, S.C.; et al. Understanding High-Dose, Ultra-High Dose Rate, and Spatially Fractionated Radiation Therapy. *Int. J. Radiat. Oncol. Biol. Phys.* **2020**, *107*, 766–778. [CrossRef]
2. Prezado, Y.; Grams, M.; Jouglar, E.; Martinez-Rovira, I.; Ortiz, R.; Seco, J.; Chang, S. Spatially fractionated radiation therapy: A critical review on current status of clinical and preclinical studies and knowledge gaps. *Phys. Med. Biol.* **2024**, *69*, 10TR02. [CrossRef]
3. Billena, C.; Khan, A.J. A Current Review of Spatial Fractionation: Back to the Future? *Int. J. Radiat. Oncol. Biol. Phys.* **2019**, *104*, 177–187. [CrossRef]
4. Yan, W.; Khan, M.K.; Wu, X.; Simone, C.B., 2nd; Fan, J.; Gressen, E.; Zhang, X.; Limoli, C.L.; Bahig, H.; Tubin, S.; et al. Spatially fractionated radiation therapy: History, present and the future. *Clin. Transl. Radiat. Oncol.* **2020**, *20*, 30–38. [CrossRef] [PubMed]
5. Amendola, B.E.; Perez, N.C.; Mayr, N.A.; Wu, X.; Amendola, M. Spatially Fractionated Radiation Therapy Using Lattice Radiation in Far-advanced Bulky Cervical Cancer: A Clinical and Molecular Imaging and Outcome Study. *Radiat. Res.* **2020**, *194*, 724–736. [CrossRef] [PubMed]
6. Duriseti, S.; Kavanaugh, J.; Goddu, S.; Price, A.; Knutson, N.; Reynoso, F.; Michalski, J.; Mutic, S.; Robinson, C.; Spraker, M.B. Spatially fractionated stereotactic body radiation therapy (Lattice) for large tumors. *Adv. Radiat. Oncol.* **2021**, *6*, 100639. [CrossRef]
7. Mohiuddin, M.; Fujita, M.; Regine, W.F.; Megooni, A.S.; Ibbott, G.S.; Ahmed, M.M. High-dose spatially-fractionated radiation (GRID): A new paradigm in the management of advanced cancers. *Int. J. Radiat. Oncol. Biol. Phys.* **1999**, *45*, 721–727. [CrossRef] [PubMed]
8. Zwicker, R.D.; Meigooni, A.; Mohiuddin, M. Therapeutic advantage of grid irradiation for large single fractions. *Int. J. Radiat. Oncol. Biol. Phys.* **2004**, *58*, 1309–1315. [CrossRef] [PubMed]

9. Huhn, J.L.; Regine, W.F.; Valentino, J.P.; Meigooni, A.S.; Kudrimoti, M.; Mohiuddin, M. Spatially fractionated GRID radiation treatment of advanced neck disease associated with head and neck cancer. *Technol. Cancer Res. Treat.* **2006**, *5*, 607–612. [CrossRef] [PubMed]
10. Neuner, G.; Mohiuddin, M.M.; Vander Walde, N.; Goloubeva, O.; Ha, J.; Yu, C.X.; Regine, W.F. High-dose spatially fractionated GRID radiation therapy (SFGRT): A comparison of treatment outcomes with Cerrobend vs. MLC SFGRT. *Int. J. Radiat. Oncol. Biol. Phys.* **2012**, *82*, 1642–1649. [CrossRef] [PubMed]
11. Narayanasamy, G.; Zhang, X.; Meigooni, A.; Paudel, N.; Morrill, S.; Maraboyina, S.; Peacock, L.; Penagaricano, J. Therapeutic benefits in grid irradiation on Tomotherapy for bulky, radiation-resistant tumors. *Acta Oncol.* **2017**, *56*, 1043–1047. [CrossRef]
12. Choi, J.I.; Daniels, J.; Cohen, D.; Li, Y.; Ha, C.S.; Eng, T.Y. Clinical Outcomes of Spatially Fractionated GRID Radiotherapy in the Treatment of Bulky Tumors of the Head and Neck. *Cureus* **2019**, *11*, e4637. [CrossRef]
13. Schultke, E.; Balosso, J.; Breslin, T.; Cavaletti, G.; Djonov, V.; Esteve, F.; Grotzer, M.; Hildebrandt, G.; Valdman, A.; Laissue, J. Microbeam radiation therapy—Grid therapy and beyond: A clinical perspective. *Br. J. Radiol.* **2017**, *90*, 20170073. [CrossRef]
14. Dilmanian, F.A.; Button, T.M.; Le Duc, G.; Zhong, N.; Pena, L.A.; Smith, J.A.; Martinez, S.R.; Bacarian, T.; Tammam, J.; Ren, B.; et al. Response of rat intracranial 9L gliosarcoma to microbeam radiation therapy. *Neuro-Oncology* **2002**, *4*, 26–38. [CrossRef]
15. Bouchet, A.; Lemasson, B.; Le Duc, G.; Maisin, C.; Brauer-Krisch, E.; Siegbahn, E.A.; Renaud, L.; Khalil, E.; Remy, C.; Poillot, C.; et al. Preferential effect of synchrotron microbeam radiation therapy on intracerebral 9L gliosarcoma vascular networks. *Int. J. Radiat. Oncol. Biol. Phys.* **2010**, *78*, 1503–1512. [CrossRef] [PubMed]
16. Prezado, Y.; Sarun, S.; Gil, S.; Deman, P.; Bouchet, A.; Le Duc, G. Increase of lifespan for glioma-bearing rats by using minibeam radiation therapy. *J. Synchrotron Radiat.* **2012**, *19*, 60–65. [CrossRef] [PubMed]
17. Bertho, A.; Iturri, L.; Brisebard, E.; Juchaux, M.; Gilbert, C.; Ortiz, R.; Sebrie, C.; Jourdain, L.; Lamirault, C.; Ramasamy, G.; et al. Evaluation of the Role of the Immune System Response After Minibeam Radiation Therapy. *Int. J. Radiat. Oncol. Biol. Phys.* **2023**, *115*, 426–439. [CrossRef] [PubMed]
18. Sotiropoulos, M.; Brisebard, E.; Le Dudal, M.; Jouvion, G.; Juchaux, M.; Crepin, D.; Sebrie, C.; Jourdain, L.; Labiod, D.; Lamirault, C.; et al. X-rays minibeam radiation therapy at a conventional irradiator: Pilot evaluation in F98-glioma bearing rats and dose calculations in a human phantom. *Clin. Transl. Radiat. Oncol.* **2021**, *27*, 44–49. [CrossRef]
19. Grams, M.; Mateus, C.Q.; Mashayekhi, M.; Mutter, R.W.; Djonov, V.; Fazzari, J.; Xiao, H.; Frechette, K.M.; Wenworth, A.J.; Morris, J.M.; et al. Minibeam Radiation Therapy Treatment (MBRT): Commissioning and First Clinical Implementation. *Int. J. Radiat. Biol.* **2024**, *120*, 1423–1434. [CrossRef]
20. Deman, P.; Vautrin, M.; Edouard, M.; Stupar, V.; Bobyk, L.; Farion, R.; Elleaume, H.; Remy, C.; Barbier, E.L.; Esteve, F.; et al. Monochromatic minibeams radiotherapy: From healthy tissue-sparing effect studies toward first experimental glioma bearing rats therapy. *Int. J. Radiat. Oncol. Biol. Phys.* **2012**, *82*, e693–e700. [CrossRef] [PubMed]
21. Prezado, Y.; Deman, P.; Varlet, P.; Jouvion, G.; Gil, S.; Le Clec, H.C.; Bernard, H.; Le Duc, G.; Sarun, S. Tolerance to Dose Escalation in Minibeam Radiation Therapy Applied to Normal Rat Brain: Long-Term Clinical, Radiological and Histopathological Analysis. *Radiat. Res.* **2015**, *184*, 314–321. [CrossRef]
22. Dilmanian, F.A.; Zhong, Z.; Bacarian, T.; Benveniste, H.; Romanelli, P.; Wang, R.; Welwart, J.; Yuasa, T.; Rosen, E.M.; Anschel, D.J. Interlaced X-ray microplanar beams: A radiosurgery approach with clinical potential. *Proc. Natl. Acad. Sci. USA* **2006**, *103*, 9709–9714. [CrossRef] [PubMed]
23. Prezado, Y.; Jouvion, G.; Hardy, D.; Patriarca, A.; Nauraye, C.; Bergs, J.; Gonzalez, W.; Guardiola, C.; Juchaux, M.; Labiod, D.; et al. Proton Minibeam Radiation Therapy Spares Normal Rat Brain: Long-Term Clinical, Radiological and Histopathological Analysis. *Sci. Rep.* **2017**, *7*, 14403. [CrossRef]
24. Girst, S.; Greubel, C.; Reindl, J.; Siebenwirth, C.; Zlobinskaya, O.; Walsh, D.W.M.; Ilicic, K.; Aichler, M.; Walch, A.; Wilkens, J.J.; et al. Proton Minibeam Radiation Therapy Reduces Side Effects in an In Vivo Mouse Ear Model. *Int. J. Radiat. Oncol. Biol. Phys.* **2016**, *95*, 234–241. [CrossRef] [PubMed]
25. Zlobinskaya, O.; Girst, S.; Greubel, C.; Hable, V.; Siebenwirth, C.; Walsh, D.W.; Multhoff, G.; Wilkens, J.J.; Schmid, T.E.; Dollinger, G. Reduced side effects by proton microchannel radiotherapy: Study in a human skin model. *Radiat. Environ. Biophys.* **2013**, *52*, 123–133. [CrossRef]
26. Lamirault, C.; Doyere, V.; Juchaux, M.; Pouzoulet, F.; Labiod, D.; Dendale, R.; Patriarca, A.; Nauraye, C.; Le Dudal, M.; Jouvion, G.; et al. Short and long-term evaluation of the impact of proton minibeam radiation therapy on motor, emotional and cognitive functions. *Sci. Rep.* **2020**, *10*, 13511. [CrossRef]
27. Prezado, Y.; Dos Santos, M.; Gonzalez, W.; Jouvion, G.; Guardiola, C.; Heinrich, S.; Labiod, D.; Juchaux, M.; Jourdain, L.; Sebrie, C.; et al. Transfer of Minibeam Radiation Therapy into a cost-effective equipment for radiobiological studies: A proof of concept. *Sci. Rep.* **2017**, *7*, 17295. [CrossRef] [PubMed]
28. Prezado, Y.; Jouvion, G.; Patriarca, A.; Nauraye, C.; Guardiola, C.; Juchaux, M.; Lamirault, C.; Labiod, D.; Jourdain, L.; Sebrie, C.; et al. Proton minibeam radiation therapy widens the therapeutic index for high-grade gliomas. *Sci. Rep.* **2018**, *8*, 16479. [CrossRef] [PubMed]

29. Lamirault, C.; Brisebard, E.; Patriarca, A.; Juchaux, M.; Crepin, D.; Labiod, D.; Pouzoulet, F.; Sebrie, C.; Jourdain, L.; Le Dudal, M.; et al. Spatially Modulated Proton Minibeams Results in the Same Increase of Lifespan as a Uniform Target Dose Coverage in F98-Glioma-Bearing Rats. *Radiat. Res.* **2020**, *194*, 715–723. [CrossRef] [PubMed]
30. Prezado, Y.; Jouvion, G.; Guardiola, C.; Gonzalez, W.; Juchaux, M.; Bergs, J.; Nauraye, C.; Labiod, D.; De Marzi, L.; Pouzoulet, F.; et al. Tumor Control in RG2 Glioma-Bearing Rats: A Comparison Between Proton Minibeam Therapy and Standard Proton Therapy. *Int. J. Radiat. Oncol. Biol. Phys.* **2019**, *104*, 266–271. [CrossRef] [PubMed]
31. Bertho, A.; Ortiz, R.; Juchaux, M.; Gilbert, C.; Lamirault, C.; Pouzoulet, F.; Polledo, L.; Liens, A.; Warfving, N.; Sebrie, C.; et al. First Evaluation of Temporal and Spatial Fractionation in Proton Minibeam Radiation Therapy of Glioma-Bearing Rats. *Cancers* **2021**, *13*, 4865. [CrossRef] [PubMed]
32. Moghaddasi, L.; Reid, P.; Bezak, E.; Marcu, L.G. Radiobiological and Treatment-Related Aspects of Spatially Fractionated Radiotherapy. *Int. J. Mol. Sci.* **2022**, *23*, 3366. [CrossRef] [PubMed]
33. Asur, R.; Butterworth, K.T.; Penagaricano, J.A.; Prise, K.M.; Griffin, R.J. High dose bystander effects in spatially fractionated radiation therapy. *Cancer Lett.* **2015**, *356*, 52–57. [CrossRef] [PubMed]
34. Fernandez-Palomo, C.; Schultke, E.; Smith, R.; Brauer-Krisch, E.; Laissue, J.; Schroll, C.; Fazzari, J.; Seymour, C.; Mothersill, C. Bystander effects in tumor-free and tumor-bearing rat brains following irradiation by synchrotron X-rays. *Int. J. Radiat. Biol.* **2013**, *89*, 445–453. [CrossRef] [PubMed]
35. Fontanella, A.N.; Boss, M.K.; Hadsell, M.; Zhang, J.; Schroeder, T.; Berman, K.G.; Dewhirst, M.W.; Chang, S.; Palmer, G.M. Effects of high-dose microbeam irradiation on tumor microvascular function and angiogenesis. *Radiat. Res.* **2015**, *183*, 147–158. [CrossRef]
36. Bouchet, A.; Serduc, R.; Laissue, J.A.; Djonov, V. Effects of microbeam radiation therapy on normal and tumoral blood vessels. *Phys. Med.* **2015**, *31*, 634–641. [CrossRef] [PubMed]
37. Dilmanian, F.A.; Qu, Y.; Feinendegen, L.E.; Pena, L.A.; Bacarian, T.; Henn, F.A.; Kalef-Ezra, J.; Liu, S.; Zhong, Z.; McDonald, J.W. Tissue-sparing effect of X-ray microplanar beams particularly in the CNS: Is a bystander effect involved? *Exp. Hematol.* **2007**, *35*, 69–77. [CrossRef] [PubMed]
38. Sathishkumar, S.; Boyanovsky, B.; Karakashian, A.A.; Rozenova, K.; Giltiay, N.V.; Kudrimoti, M.; Mohiuddin, M.; Ahmed, M.M.; Nikolova-Karakashian, M. Elevated sphingomyelinase activity and ceramide concentration in serum of patients undergoing high dose spatially fractionated radiation treatment: Implications for endothelial apoptosis. *Cancer Biol. Ther.* **2005**, *4*, 979–986. [CrossRef]
39. Griffin, R.J.; Koonce, N.A.; Dings, R.P.; Siegel, E.; Moros, E.G.; Brauer-Krisch, E.; Corry, P.M. Microbeam radiation therapy alters vascular architecture and tumor oxygenation and is enhanced by a galectin-1 targeted anti-angiogenic peptide. *Radiat. Res.* **2012**, *177*, 804–812. [CrossRef]
40. Yang, Y.; Swierczak, A.; Ibahim, M.; Paiva, P.; Cann, L.; Stevenson, A.W.; Crosbie, J.C.; Anderson, R.L.; Rogers, P.A.W. Synchrotron microbeam radiotherapy evokes a different early tumor immunomodulatory response to conventional radiotherapy in EMT6.5 mammary tumors. *Radiother. Oncol.* **2019**, *133*, 93–99. [CrossRef]
41. Smilowitz, H.M.; Blattmann, H.; Brauer-Krisch, E.; Bravin, A.; Di Michiel, M.; Gebbers, J.O.; Hanson, A.L.; Lyubimova, N.; Slatkin, D.N.; Stepanek, J.; et al. Synergy of gene-mediated immunoprophylaxis and microbeam radiation therapy for advanced intracerebral rat 9L gliosarcomas. *J. Neuro-Oncol.* **2006**, *78*, 135–143. [CrossRef]
42. Bouchet, A.; Sakakini, N.; El Atifi, M.; Le Clec'h, C.; Brauer, E.; Moisan, A.; Deman, P.; Rihet, P.; Le Duc, G.; Pelletier, L. Early gene expression analysis in 9L orthotopic tumor-bearing rats identifies immune modulation in molecular response to synchrotron microbeam radiation therapy. *PLoS ONE* **2013**, *8*, e81874. [CrossRef] [PubMed]
43. Mohiuddin, M.; Park, H.; Hallmeyer, S.; Richards, J. High-Dose Radiation as a Dramatic, Immunological Primer in Locally Advanced Melanoma. *Cureus* **2015**, *7*, e417. [CrossRef] [PubMed]
44. Kanagavelu, S.; Gupta, S.; Wu, X.; Philip, S.; Wattenberg, M.M.; Hodge, J.W.; Couto, M.D.; Chung, K.D.; Ahmed, M.M. In vivo effects of lattice radiation therapy on local and distant lung cancer: Potential role of immunomodulation. *Radiat. Res.* **2014**, *182*, 149–162. [CrossRef] [PubMed]
45. Tubin, S.; Popper, H.H.; Brcic, L. Novel stereotactic body radiation therapy (SBRT)-based partial tumor irradiation targeting hypoxic segment of bulky tumors (SBRT-PATHY): Improvement of the radiotherapy outcome by exploiting the bystander and abscopal effects. *Radiat. Oncol.* **2019**, *14*, 21. [CrossRef]
46. Rodriguez-Ruiz, M.E.; Vanpouille-Box, C.; Melero, I.; Formenti, S.C.; Demaria, S. Immunological Mechanisms Responsible for Radiation-Induced Abscopal Effect. *Trends Immunol.* **2018**, *39*, 644–655. [CrossRef] [PubMed]
47. Chmura, S.J.; Connell, P.P.; Weichselbaum, R.R. Retuning the Radio in Radiobiology. *J. Natl. Cancer Inst.* **2018**, *110*, 325–326. [CrossRef]
48. Kirsch, D.G.; Diehn, M.; Kesarwala, A.H.; Maity, A.; Morgan, M.A.; Schwarz, J.K.; Bristow, R.; Demaria, S.; Eke, I.; Griffin, R.J.; et al. The Future of Radiobiology. *J. Natl. Cancer Inst.* **2018**, *110*, 329–340. [CrossRef] [PubMed]

49. Formenti, S.C.; Demaria, S. Radiation therapy to convert the tumor into an in situ vaccine. *Int. J. Radiat. Oncol. Biol. Phys.* **2012**, *84*, 879–880. [CrossRef] [PubMed]
50. Formenti, S.C.; Demaria, S. Combining radiotherapy and cancer immunotherapy: A paradigm shift. *J. Natl. Cancer Inst.* **2013**, *105*, 256–265. [CrossRef] [PubMed]
51. Golden, E.B.; Chhabra, A.; Chachoua, A.; Adams, S.; Donach, M.; Fenton-Kerimian, M.; Friedman, K.; Ponzo, F.; Babb, J.S.; Goldberg, J.; et al. Local radiotherapy and granulocyte-macrophage colony-stimulating factor to generate abscopal responses in patients with metastatic solid tumours: A proof-of-principle trial. *Lancet Oncol.* **2015**, *16*, 795–803. [CrossRef] [PubMed]
52. Vanpouille-Box, C.; Pilones, K.A.; Wennerberg, E.; Formenti, S.C.; Demaria, S. In situ vaccination by radiotherapy to improve responses to anti-CTLA-4 treatment. *Vaccine* **2015**, *33*, 7415–7422. [CrossRef]
53. Dimberu, P.M.; Leonhardt, R.M. Cancer immunotherapy takes a multi-faceted approach to kick the immune system into gear. *Yale J. Biol. Med.* **2011**, *84*, 371–380. [PubMed]
54. Rivera, J.N.; Kierski, T.M.; Kasoji, S.K.; Abrantes, A.S.; Dayton, P.A.; Chang, S.X. Conventional dose rate spatially-fractionated radiation therapy (SFRT) treatment response and its association with dosimetric parameters-A preclinical study in a Fischer 344 rat model. *PLoS ONE* **2020**, *15*, e0229053. [CrossRef] [PubMed]
55. Casey, A.E.; Ross, G.L.; Langston, R.R. Selective XYZ factor in C57 black mammary carcinoma Eo771. *Proc. Soc. Exp. Biol. Med.* **1949**, *72*, 83–89. [CrossRef] [PubMed]
56. Dunham, L.J.; Stewart, H.L. A survey of transplantable and transmissible animal tumors. *J. Natl. Cancer Inst.* **1953**, *13*, 1299–1377.
57. Johnstone, C.N.; Smith, Y.E.; Cao, Y.; Burrows, A.D.; Cross, R.S.; Ling, X.; Redvers, R.P.; Doherty, J.P.; Eckhardt, B.L.; Natoli, A.L.; et al. Functional and molecular characterisation of EO771.LMB tumours, a new C57BL/6-mouse-derived model of spontaneously metastatic mammary cancer. *Dis. Model. Mech.* **2015**, *8*, 237–251. [CrossRef] [PubMed]
58. Betof, A.S.; Lascola, C.D.; Weitzel, D.; Landon, C.; Scarbrough, P.M.; Devi, G.R.; Palmer, G.; Jones, L.W.; Dewhirst, M.W. Modulation of murine breast tumor vascularity, hypoxia and chemotherapeutic response by exercise. *J. Natl. Cancer Inst.* **2015**, *107*, djv040. [CrossRef] [PubMed]
59. Faustino-Rocha, A.; Oliveira, P.A.; Pinho-Oliveira, J.; Teixeira-Guedes, C.; Soares-Maia, R.; da Costa, R.G.; Colaco, B.; Pires, M.J.; Colaco, J.; Ferreira, R.; et al. Estimation of rat mammary tumor volume using caliper and ultrasonography measurements. *Lab Anim.* **2013**, *42*, 217–224. [CrossRef]
60. Mayr, N.A.; Mohiuddin, M.; Snider, J.W.; Zhang, H.; Griffin, R.J.; Amendola, B.E.; Hippe, D.S.; Perez, N.C.; Wu, X.; Lo, S.S.; et al. Practice Patterns of Spatially Fractionated Radiation Therapy: A Clinical Practice Survey. *Adv. Radiat. Oncol.* **2024**, *9*, 101308. [CrossRef] [PubMed]
61. Dewan, M.Z.; Galloway, A.E.; Kawashima, N.; Dewyngaert, J.K.; Babb, J.S.; Formenti, S.C.; Demaria, S. Fractionated but not single-dose radiotherapy induces an immune-mediated abscopal effect when combined with anti-CTLA-4 antibody. *Clin. Cancer. Res.* **2009**, *15*, 5379–5388. [CrossRef]
62. Demaria, S.; Guha, C.; Schoenfeld, J.; Morris, Z.; Monjazeb, A.; Sikora, A.; Crittenden, M.; Shiao, S.; Khleif, S.; Gupta, S.; et al. Radiation dose and fraction in immunotherapy: One-size regimen does not fit all settings, so how does one choose? *J. Immunother. Cancer* **2021**, *9*, e002038. [CrossRef]
63. Gandhi, S.J.; Minn, A.J.; Vonderheide, R.H.; Wherry, E.J.; Hahn, S.M.; Maity, A. Awakening the immune system with radiation: Optimal dose and fractionation. *Cancer Lett.* **2015**, *368*, 185–190. [CrossRef]
64. Zeng, J.; See, A.P.; Phallen, J.; Jackson, C.M.; Belcaid, Z.; Ruzevick, J.; Durham, N.; Meyer, C.; Harris, T.J.; Albesiano, E.; et al. Anti-PD-1 blockade and stereotactic radiation produce long-term survival in mice with intracranial gliomas. *Int. J. Radiat. Oncol. Biol. Phys.* **2013**, *86*, 343–349. [CrossRef]
65. Deng, L.; Liang, H.; Burnette, B.; Beckett, M.; Darga, T.; Weichselbaum, R.R.; Fu, Y.X. Irradiation and anti-PD-L1 treatment synergistically promote antitumor immunity in mice. *J. Clin. Investig.* **2014**, *124*, 687–695. [CrossRef] [PubMed]
66. Park, I.H.; Kong, S.Y.; Ro, J.Y.; Kwon, Y.; Kang, J.H.; Mo, H.J.; Jung, S.Y.; Lee, S.; Lee, K.S.; Kang, H.S.; et al. Prognostic Implications of Tumor-Infiltrating Lymphocytes in Association with Programmed Death Ligand 1 Expression in Early-Stage Breast Cancer. *Clin. Breast Cancer* **2016**, *16*, 51–58. [CrossRef] [PubMed]
67. Twyman-Saint Victor, C.; Rech, A.J.; Maity, A.; Rengan, R.; Pauken, K.E.; Stelekati, E.; Benci, J.L.; Xu, B.; Dada, H.; Odorizzi, P.M.; et al. Radiation and dual checkpoint blockade activate non-redundant immune mechanisms in cancer. *Nature* **2015**, *520*, 373–377. [CrossRef] [PubMed]
68. Mali, S.B. Mini review of spatially fractionated radiation therapy for cancer management. *Oral Oncol. Rep.* **2024**, *9*, 100175. [CrossRef]
69. Zhang, Z.; Liu, X.; Chen, D.; Yu, J. Radiotherapy combined with immunotherapy: The dawn of cancer treatment. *Signal Transduct. Target. Ther.* **2022**, *7*, 258. [CrossRef] [PubMed]
70. Fernandez-Palomo, C.; Chang, S.; Prezado, Y. Should Peak Dose Be Used to Prescribe Spatially Fractionated Radiation Therapy?—A Review of Preclinical Studies. *Cancers* **2022**, *14*, 3625. [CrossRef] [PubMed]

71. Zhang, H.; Wu, X.; Zhang, X.; Chang, S.X.; Megooni, A.; Donnelly, E.D.; Ahmed, M.M.; Griffin, R.J.; Welsh, J.S.; Simone, C.B., 2nd; et al. Photon GRID Radiation Therapy: A Physics and Dosimetry White Paper from the Radiosurgery Society (RSS) GRID/LATTICE, Microbeam and FLASH Radiotherapy Working Group. *Radiat. Res.* **2020**, *194*, 665–677. [CrossRef]
72. Wu, X.; Perez, N.C.; Zheng, Y.; Li, X.; Jiang, L.; Amendola, B.E.; Xu, B.; Mayr, N.A.; Lu, J.J.; Hatoum, G.F.; et al. The Technical and Clinical Implementation of LATTICE Radiation Therapy (LRT). *Radiat. Res.* **2020**, *194*, 737–746. [CrossRef]

Disclaimer/Publisher's Note: The statements, opinions and data contained in all publications are solely those of the individual author(s) and contributor(s) and not of MDPI and/or the editor(s). MDPI and/or the editor(s) disclaim responsibility for any injury to people or property resulting from any ideas, methods, instructions or products referred to in the content.